Hindawi
Advances in Civil Engineering
Volume 2018, Article ID 7179831, 12 pages
https://doi.org/10.1155/2018/7179831

Research Article

Influence of Fissure Number on the Mechanical Properties of Layer-Crack Rock Models under Uniaxial Compression

Yun-liang Tan,[1,2,3] **Wei-yao Guo**,[1,2,3] **Tong-bin Zhao**,[1,2,3] **Feng-hai Yu**,[1,2,3] **Bin Huang**,[1,2] **and Dong-mei Huang**[1,2]

[1]*State Key Laboratory of Mining Disaster Prevention and Control Co-founded by Shandong Province and the Ministry of Science and Technology, Shandong University of Science and Technology, Qingdao 266590, China*
[2]*College of Mining and Safety Engineering, Shandong University of Science and Technology, Qingdao 266590, China*
[3]*National Demonstration Center for Experimental Mining Engineering Education, Shandong University of Science and Technology, Qingdao 266590, China*

Correspondence should be addressed to Wei-yao Guo; 363216782@qq.com and Feng-hai Yu; yufenghai2006@163.com

Received 28 August 2017; Accepted 4 March 2018; Published 9 May 2018

Academic Editor: Ottavia Corbi

Many case studies have revealed that rock bursts generally occur in the high stress concentration area where layer-crack structures often exist, especially for brittle coal or rock masses. Understanding the mechanical properties of layer-crack rock models is beneficial for rational design and stability analysis of rock engineering project and rock burst prevention. This study experimentally investigated the influence of fissure number on the mechanical properties of layer-crack rock models through uniaxial compression tests. The digital speckle correlation method (DSCM) and acoustic emission (AE) techniques were applied to record and analyze the information of deformation and failure processes. Test results show the following: the bearing capacity of layer-crack specimen decreases compared with intact specimen, but their failure modes are similar, which are the splitting failure accompanied with local shear failure; the nonuniform deformation phenomenon begins to appear at the elastic deformation stage for layer-crack specimens; the AE behavior of intact specimens consists of three stages, that is, active stage, quiet stage, and major active stage, but for layer-crack specimens, it is characteristic by three peaks without quiet stage. In addition, as the fissure number of layer-crack specimens increases, the bearing capacity of specimens decreases, the appearing time of nonuniform deformation phenomenon in the specimen surface decreases, the AE events are denser and denser in each peak stage, and the risk of dynamic instability of layer-crack structure increases. At last, the failure mechanism of layer-crack structure and the related mitigation advices were discussed based on the test results. In general, the novelty is that this paper focuses on the failure mechanism of layer-crack structure directly.

1. Introduction

With the worldwide economic and social development, the shallow mineral resources are gradually depleted, and the depth of mining or tunnelling is deeper and deeper [1–5]. Under the influence of excavation unloading condition, the deformation and failure modes of deep rock mass are different from those of shallow rock mass, which shows obvious discontinuous and nonlinear characteristics [6–10]. Phenomena of layer-crack structure, zonal disintegration, rock burst, large deformation, and so on increase in deep exploitation. The layer-crack structures refer to spalling and slabbing structures of surrounding rock before the occurrence of rock bursts in this paper. Case studies have revealed that lots of rock bursts occurred in the high stress concentration area where layer-crack structures exist, as shown in Figure 1 [11–15]. Figures 1(a) and 1(b) show the phenomena of layer-crack structures in brittle rock mass, and Figures 1(c) and 1(d) show the phenomena of layer-crack structures in brittle coal mass. In general, layer-crack structures are closely related with the occurrence of rock bursts in brittle rock or coal mass.

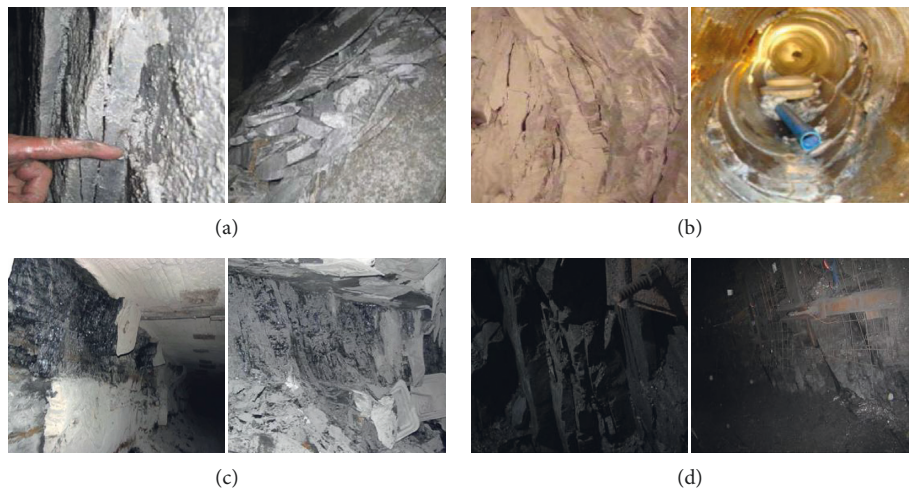

Figure 1: Phenomena of layer-crack structures in coal mines and tunnels. Layer-crack phenomenon in (a) tunnel A [11], (b) tunnel B [12], (c) coal mine A [13], and (d) coal mine B.

Regarding research on brittle rock mass, theoretical analysis, numerical modeling, laboratory test, and field monitoring methods have been used to study the layer-crack structure and rock burst. In aspect of theoretical analysis, Stacey [16] proposed a simple and empirical criterion for fracture initiation in brittle rock and explained the phenomenon of layer-crack structure formation; Hou et al. [17] theoretically discussed the occurrence mechanism of layer-crack rock bursts; Qiu et al. [18] proposed a comprehensive velocity assessment method to evaluate the rock burst wall-rock velocity evoked by rock slab flexure sources; and Weng et al. [19] analyzed the occurrence mechanism and time-dependency effect of layer-crack rock bursts based on the three-parameter viscoelasticity constitutive relationship and the slabbing thin plate mechanical model. In aspect of numerical modeling, Cai [20] concluded that the generation of tunnel surface parallel fractures and microcracks was attributed to material heterogeneity and the existence of relatively high intermediate principal stress, as well as zero to low minimum principal stress confinement, and Zhang et al. [21] analyzed the influence of intermediate principal stress, stress path, and principal stress axes rotation on the failure mechanism of layer-crack structure using numerical simulation. In aspect of laboratory test, numerous studies investigated the mechanical response of rocks to various loading and unloading conditions, and many layer-crack phenomena before rock bursts in different rocks were reported. For example, He et al. [22, 23] divided the process of granite rock burst into four stages and analyzed the AE characteristics during the burst process of limestone through single-face dynamic unloading tests; Gong et al. [11] found that the process of rock burst and the layer-crack failure phenomenon of experimental rock samples were in good accordance with field observations; Zhao et al. [24] studied the influence of unloading rate on the characteristics of strain burst, and test results showed that the layer-crack phenomenon was influenced by the unloading rate; and Du et al. [25] summarized the main triaxial loading and unloading tests methods for determining the mechanical behavior of rock materials and researched the layer-crack phenomenon and rock burst induced by true-triaxial unloading and local dynamic disturbance.

Regarding research on brittle coal mass, scholars also have conducted significant work on the layer-crack phenomenon and rock burst. For example, Zhang et al. [26, 27] found that the occurrence of rock burst in Sanhejian Coal Mine was local instability related to the layer-crack structure and analyzed the formation of layer-crack structure through fracture mechanics and laboratory tests; Peng and Lu [28] studied the formation and failure of layer-crack structure of surrounding rock under the influence of stress waves using LS-DYNA software; Bai et al. [29] presented three numerical models, that is, intact coal wall, coal wall including vertical discontinuities, and coal wall including criss-cross discontinuities, to investigate the failure mechanism of layer-crack structure of the coal wall based on extensive field surveys; and Mohamed et al. [13] found that there exist obvious layer-crack structures in the coal wall face through analyzing the current rib support practices in twenty coal mines in the USA.

As a consequence of the above researches, the meaningful results provide a good reference for understanding the mechanisms of layer-crack structure formation and rock burst occurrence. Although the viewpoint that layer-crack structures often exist before the occurrence of rock bursts is widely accepted by scholars, above researches mainly focus on the formation of layer-crack structure and the related influencing factors. There is less literature trying to study the failure mechanism of layer-crack structure through laboratory test. Therefore, four kinds of layer-crack rock models were established in this study for investigating the influence of fissure number on the mechanical properties of layer-crack rock models through uniaxial compression tests. During the test process, the digital speckle correlation method (DSCM) and acoustic emission (AE) techniques were applied to record and analyze the information of deformation and failure processes. At last, the failure mechanism of layer-crack structure and the influence of fissure number were discussed based on the test results.

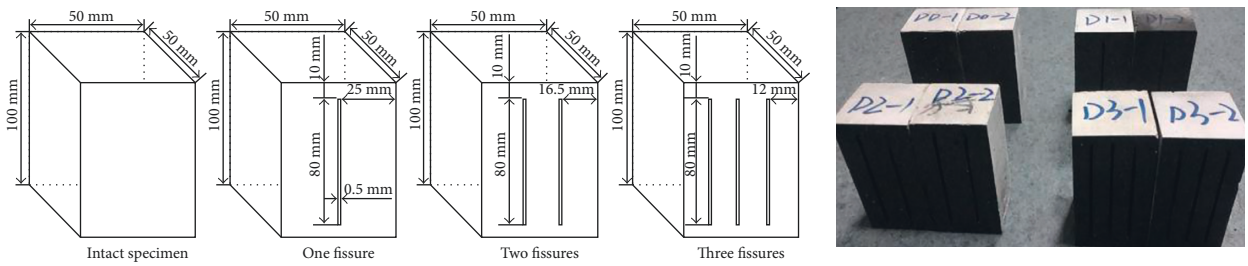

Figure 2: Sketch of test specimens. (a) Sketch of layer-crack rock models and (b) part of the test specimens.

2. Specimen Preparation and Testing

2.1. Specimen Preparation. Since it is difficult to directly fabricate joints in intact rocks, the intermittent jointed rocks are generally prepared using artificial rock-like materials in laboratory tests. In order to carry out experimental study on the mechanical properties of layer-crack models, the specimens were made of high-strength gypsum, and the water-cement ratio is 5 : 9. The reason for choosing high-strength gypsum as modeling material is that a wide range of brittle rocks can be easily prepared and the experimental results can be conventionally compared with the previous studies [30, 31]. Besides, the overall dimensions of the specimens were 50 mm wide × 100 mm height × 50 mm thickness. The height-width ratio is set to 2.0 to guarantee a uniform stress state in all specimens interior. The single fissure geometry is mainly described by three parameters: fissure length, fissure width, and fissure angle (note: the term "fissure" is used to describe the artificially created flaw or crack, and the term "crack" is adopted to describe the new fracture or failure in the loading process). Since the research object of this paper is the layer-crack rock model, the fissure angle is set to 90°. Moreover, this paper mainly researches the influence of fissure number on the mechanical properties of layer-crack rock models, the fissure length and width are all set to 80 mm and 0.5 mm, respectively, but the number of fissures varies. Four kinds of specimens were designed, including intact specimens, one fissure specimen, two fissure specimens, and three fissure specimens, as shown in Figure 2. In order to ensure the accuracy of the test, three specimens were prepared for each kind of specimen. The final results were obtained based on the consistency for two or three same specimens. We design this kind of test scheme, because the damage depth of roadway surrounding rock generally is stable and the number of layer-crack plates varies, which means that the test scheme in this study is reasonable.

2.2. Test Equipment and Procedure. The uniaxial compression experiments were conducted on an RLJW-2000 servocontrolled rock pressure testing machine at the College of Mining and Safety Engineering, Shandong University of Science and Technology [32]. This testing system can record stress and strain data automatically. To obtain the mechanical behavior of layer-crack rock models with the change of fissure number under uniaxial compression in detail, the tests were done for four kinds of specimens, as shown in Figure 2. All specimens were loaded with a strain rate of $1 \times 10^{-5} \cdot s^{-1}$. The tests were carried out under a natural state.

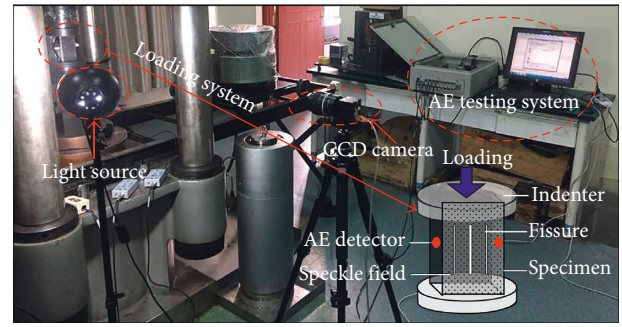

Figure 3: Experiment system.

Moreover, the digital speckle correlation method (DSCM) measurement was conducted to analyze the deformation characteristics before peak stress. DSCM is a particle-tracking method that uses digital images to evaluate full-field displacement. One side of each specimen was selected to be sprayed with black paint as underpainting and then speckled with white spots according to the DSCM method [33]. One thing needs to be explained is that if there is debris stripping in the speckle surface, the deformation fields are hard to be processed out. At the same time, the PCI-2 AE testing system (produced by American Physical Acoustic Corporation), with A/D resolution 18 bit and signal-to-noise ratio (SNR) less than 60 dB, was applied to record the AE signals. The experiment system for uniaxial compression tests is given in Figure 3.

3. Mechanical Properties of Layer-Crack Specimens under Uniaxial Compression

The axial stress-strain curves of rock-like specimens with different fissure numbers subject to uniaxial compression stress are illustrated in Figure 4. Table 1 lists the uniaxial compressive strength (σ_c), the elastic modulus (E), and the peak strain ($\varepsilon_{1\max}$) corresponding to the strain of peak stress of layer-crack specimens with different fissure numbers. In Table 1, AV is defined as the average value. From Figure 4 and Table 1, we can conclude that the fissure number greatly

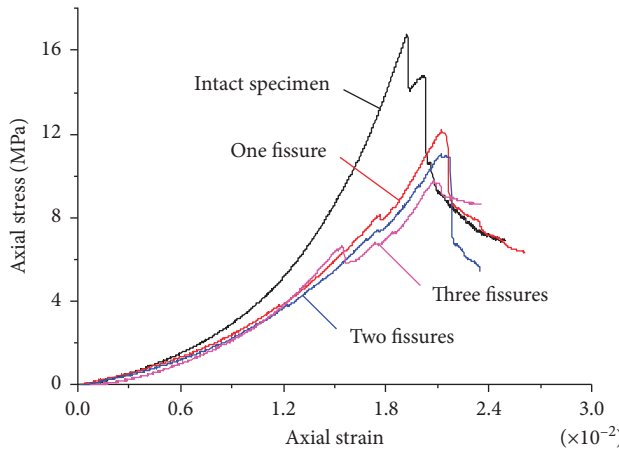

Figure 4: Axial stress-strain curves of layer-crack specimens with different fissure numbers.

Table 1: Test results of basic mechanical properties of layer-crack specimens under uniaxial compression.

Type of specimen	Specimen number	σ_c (MPa)	AV (MPa)	ε_{1max} (10^{-2})	AV (10^{-2})	E (GPa)	AV (GPa)
Intact	D0-2	16.79	16.77	1.923	1.98	2.05	1.97
	D0-3	17.39		2.050		1.99	
	D0-4	16.13		1.974		1.88	
One fissure	D1-1	12.20	12.18	2.126	2.05	1.45	1.44
	D1-3	12.01		2.071		1.38	
	D1-4	12.33		1.959		1.48	
Two fissures	D2-1	10.41	11.08	2.253	2.14	1.18	1.22
	D2-2	11.06		2.125		1.24	
	D2-3	11.77		2.036		1.23	
Three fissures	D3-1	9.21	9.11	2.040	1.93	0.89	0.90
	D3-2	9.80		2.080		0.99	
	D3-4	8.33		1.681		0.81	

affects the mechanical properties of layer-crack rock models. We will elaborate this problem in detail in the following.

3.1. Axial Stress-Strain Curves. The whole stress-strain curves consist of four stages for layer-crack specimens, including the compaction stage, elastic deformation stage, plastic deformation stage (i.e., stress stiffening and stress softening stages), and failure stage, which are similar to intact specimens, as shown in Figure 4. All the stress-strain curves experience a stress drop phenomenon after peak stress, showing brittle failure characteristics. However, the drop amplitude for intact specimens is larger than that for layer-crack specimens. The drop amplitude value for intact specimens is 7.65 MPa, but this value for layer-crack specimens varies from 0.73 to 4.01 MPa. In addition, it also illustrates that the fissure number obviously influences the mechanical properties of layer-crack specimens, that is, the uniaxial compressive strength, elastic modulus, and peak strain.

Moreover, there also exists a slight stress drop phenomenon for layer-crack specimens before reaching the peak stress. The larger the fissure number, the earlier the appearance of the slight stress drop phenomenon. For example, when the fissure number is one, two, and three, their corresponding strains are 1.77×10^{-2}, 1.68×10^{-2}, and 1.55×10^{-2}, respectively. Probably, there are two reasons causing this phenomenon. First, the layer-crack rock model is divided into multiple supporting bodies due to the existence of vertical fissures, but it is very difficult for materials to reach complete homogeneity, thus causing the incompatible deformation and asymmetric load of each supporting body during the compression process. One of the supporting bodies might enter into yield failure first while the whole layer-crack rock model still has a good bearing capacity. That is why, the slight stress drop phenomenon might appear before the complete failure of the specimen. Second, the larger the fissure number, the thinner the each supporting body of the layer-crack specimen. In other words, the bearing capacity of supporting bodies decreases as the fissure number increases. Therefore, the appearing time of slight stress drop phenomenon decreases with the increase of fissure number.

3.2. Influence on Mechanical Properties. Figure 5 shows the influence of fissure number on the mechanical parameters of layer-crack specimens, and number zero means intact specimen. Compared with intact specimens, the uniaxial compressive strength and elastic modulus of layer-crack specimens all decrease, but the variation law of peak strain is not clear. For example, the uniaxial compressive strength and elastic modulus of intact specimens are 15.9 MPa and 1.55 GPa, respectively, but they are 9.11–12.18 MPa and

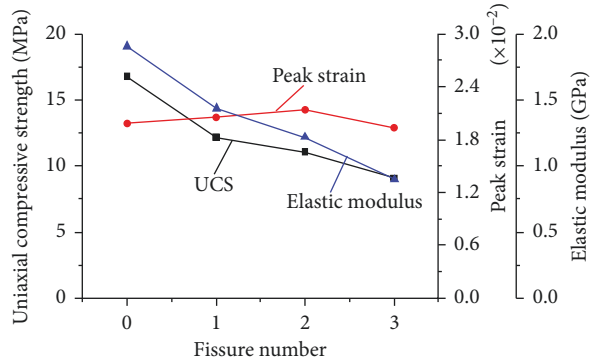

Figure 5: Influence of fissure number on the mechanical parameters of layer-crack specimens.

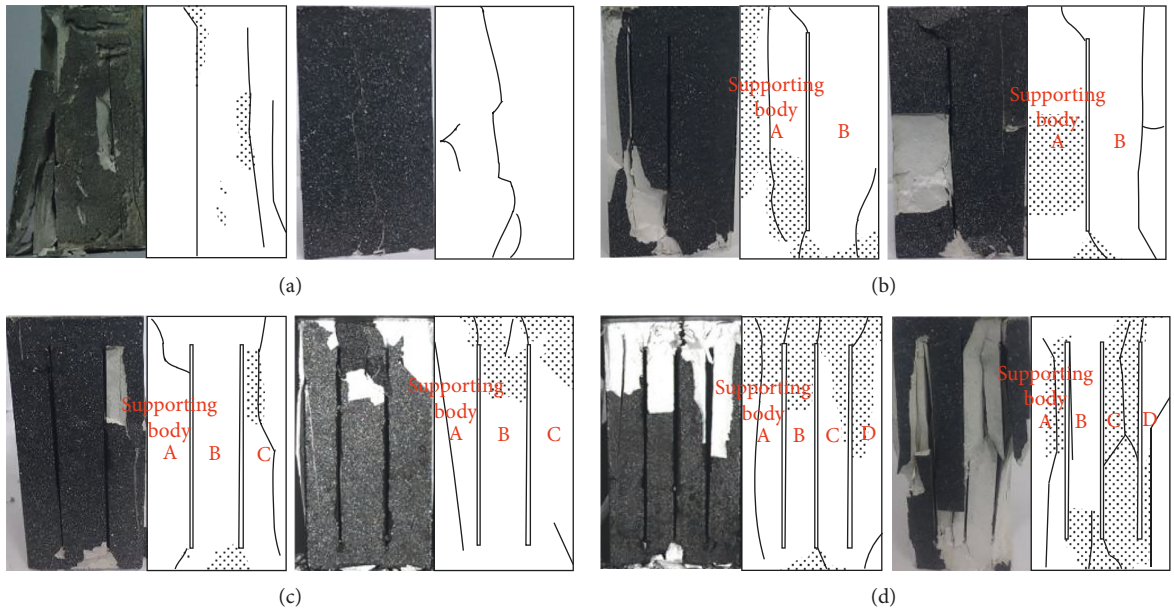

Figure 6: Failure modes of specimens: (a) intact specimen, (b) one fissure specimen, (c) two fissure specimens, and (d) three fissure specimens.

0.90–1.44 GPa for layer-crack specimens. The corresponding dropping percentages are 23.39–42.7% and 7.10–36.13%.

The fissure number influences the strength and deformation parameters of layer-crack specimens in varying degrees: when the fissure number increases, both the uniaxial compressive strength and elastic modulus decrease with the increase of fissure number, but the peak strain increases first and then decreases. Specifically speaking, when the fissure number increases from one to three, the uniaxial compressive strength and elastic modulus decrease from 12.18 MPa to 9.11 MPa and from 1.44 GPa to 0.90 GPa, respectively, whose corresponding dropping percentages are 25.21% and 37.50%. The peak strain, however, increases from 1.98×10^{-2} to 2.14×10^{-2} first and then decreases to 1.93×10^{-2} as the fissure number increases from one to three.

3.3. Influence on Failure Modes. Figure 6 shows the failure modes of intact specimens and layer-crack specimens. Splitting failure accompanied with local shear failure is the main failure mode for intact specimens, as shown in Figure 6(a). It can be seen from Figure 6(b) that the failure mode of one fissure specimen is similar to intact specimens but mainly is the splitting failure of one to two of the two supporting bodies divided by the vertical fissure. However, the failure mode of two fissure specimens is splitting failure or shear failure of one to three of the supporting bodies, as shown in Figure 6(c), which is similar to three fissure specimens. The failure mode of three fissure specimens is also splitting failure or shear failure of one to four of the supporting bodies, as shown in Figure 6(d).

In addition, it can also be seen from Figures 6(b)–6(d) that the failure of each supporting body for layer-crack specimens is stochastic. For example, the failure pattern of the left one fissure specimen is the splitting failure of supporting body A, but the right specimen is the splitting failure of supporting body B, as shown in Figure 6(b); the failure pattern of the left two fissure specimen is the splitting failure of supporting body C accompanied with the shear failure of supporting body A, but the right specimen is the splitting failure of supporting

body B accompanied with the shear failure of supporting body C, as shown in Figure 6(c). This phenomenon might be caused by the incompatible deformation and asymmetric load of each supporting body, because the layer-crack rock model could not reach complete homogeneity.

3.4. Influence on Deformation Fields. Figure 7 shows the horizontal and vertical deformation fields of intact specimens and layer-crack specimens before peak stress from the DSCM measurement. As shown in Figure 7(a), from the compaction stage to peak stress, the deformation of specimen surface for intact specimens is almost uniform. In the compaction stage, the deformation of specimen surface for layer-crack specimens is also uniform, as shown in Figures 7(b)–7(d). When entering into the elastic deformation stage, however, the deformation field of specimen surface for layer-crack specimens begins to show a nonuniform phenomenon due to the noncomplete homogeneity. This is to say, deformation gradient difference appears in the specimen surface for layer-crack specimens in the elastic deformation stage. As entering into the yield stage, the nonuniform deformation phenomenon becomes more serious.

Moreover, Figures 7(b)–7(d) also shows that the fissure number greatly affects the deformation field of layer-crack specimens, especially the appearing time of the nonuniform deformation phenomenon in the specimen surface. For example, the nonuniform deformation phenomenon appears when the axial stress reaches at 0.4–$0.6\sigma_c$ for one fissure specimen or two fissure specimens, but for three fissure specimens, this phenomenon appears when the axial stress reached at 0.2–$0.4\sigma_c$. As shown in Figures 7(c) and 7(d), the deformation field cannot be recorded at 0.8–$1.0\sigma_c$ for two fissure specimens or three fissure specimens due to this phenomenon, which might lead to debris stripping in the speckle surface of supporting bodies. In general, the DSCM results reveal that under the same loading and lithology conditions, if the number of layer-crack plate increases, the instability probability will be enhanced, that is, the occurrence risk of rock bursts increases.

3.5. Influence on AE Characteristics. According to Figure 8, a further study to look into the AE activity law of intact specimens and layer-crack specimens during the uniaxial loading process was conducted. As shown in Figure 8(a), the AE behavior of intact specimens mainly consists of three stages: minor active stage, quiet stage, and major active stage. At the beginning of the axial loading process, only a few AE events could be recorded, which is owing to the closure of primary defects. The initial AE activity process is defined as the minor active stage. As the axial load continues increasing, the AE behavior enters into the second stage, that is, the quiet stage. During this stage, the AE behavior is quite stable accompanied with the elastic deformation stage. However, the AE events continue increasing rapidly after the quiet stage, which means the AE behavior starts to enter into the major active stage. In this stage, the inner damage of the intact specimen develops, which induces the rapid increase of AE events. In general, the AE activity law of intact specimens is similar to other research results.

According to Figures 8(b)–8(d), the AE behavior pattern of layer-crack specimens is characterized by three peaks, showing a great difference with intact specimens. There also exists the minor active stage caused by the closure of primary defects before the first peak stage. However, it is worth mentioning that new cracks begin to generate during the first peak stage and that the quiet stage seems to have disappeared. A more active stage, that is, the second peak stage, just follows the first peak period, revealing that the crack growth rate is accelerated. In the second peak stage, the phenomenon of slight stress drop is more obvious except for three fissure specimens. With the continuing increase of axial load, the AE events reach the largest until the layer-crack specimen fails with an appearance of through cracks. At the same time, more and more AE events are produced during this process, and that is the third peak stage. In addition, Figures 8(b)–8(d) also reveal that the fissure number greatly influences the AE characteristics of layer-crack specimens. The AE events are denser and denser with the increase of fissure number in each peak stage, especially in the first and second peak stages. This result also might be induced by the incompatible deformation and asymmetric load of each supporting body.

4. Discussions

Scholars have reached a consensus that the layer-crack structure makes an essential contribution to rib spalling or rock burst in brittle coal or rock mass [13, 34–39]. Figure 9 illustrates the general occurrence mechanism of rock burst related to the layer-crack strucutre. The occurrence mechanism can be described as follows [40–42]: first, the layer-crack structure forms under the compression stress concentration of surrounding rock induced by the excavation unloading, as shown in Figures 9(a) and 9(b); second, the compression stress concentration further leads to the buckling deformation of layer-crack plates (i.e., rock plates divided by these vertical macro-cracks) and to the continuous accumulation of strain energy stored in layer-crack plates, as shown in Figure 9(c); third, when the strain energy stored in layer-crack plates reaches the storage limit, dynamic instability might take place under the influence of external disturbance, as shown in Figure 9(d). Although significant work has been done on the formation process of layer-crack structure and rock burst, there is little work trying to reveal the failure mechanism of layer-crack structure in detail, that is, to explain the process illustrated in Figures 9(c) and 9(d). Therefore, this section mainly tries to explain this issue.

The experimental results show that the bearing capacity of layer-crack rock models distinctly decreases compared with intact rock models, which means that the instability probability is higher for layer-crack rock models. This phenomenon is also testified by the AE results. Except for the bearing capacity, DSCM results illustrate that when entering into the elastic deformation stage, nonuniform deformation phenomenon begins to appear in the specimen surface of layer-crack specimens. However, the deformation field for intact specimens is uniform from the compaction stage to peak

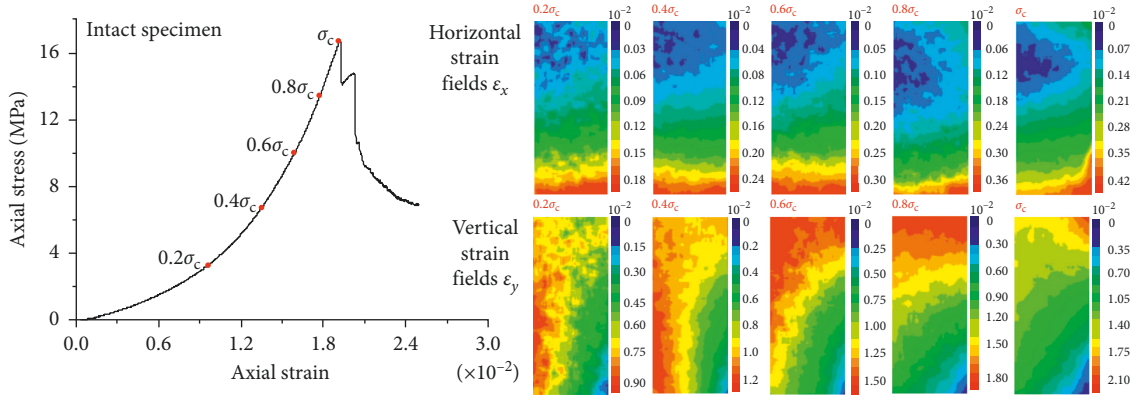

(a)

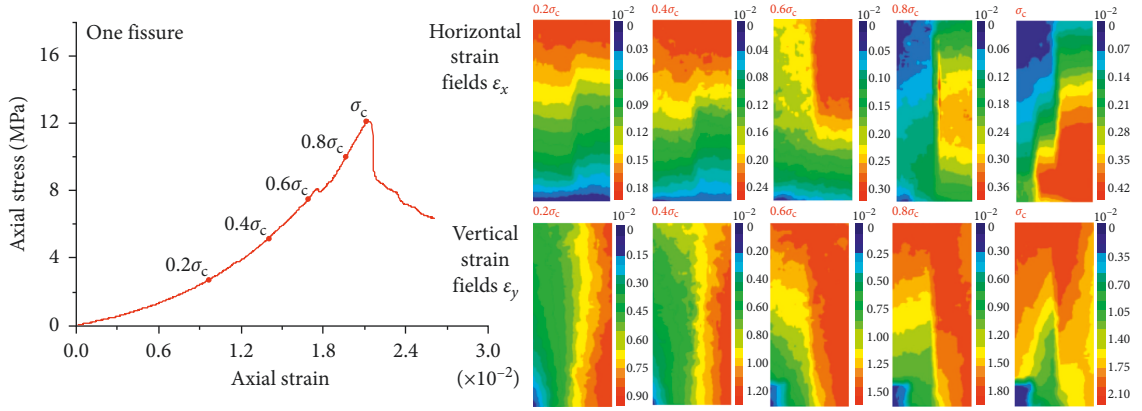

(b)

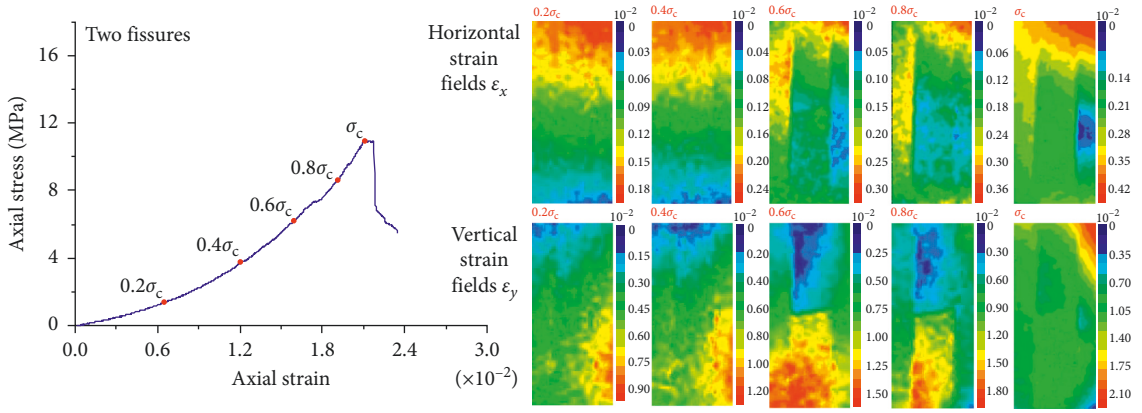

(c)

Figure 7: Continued.

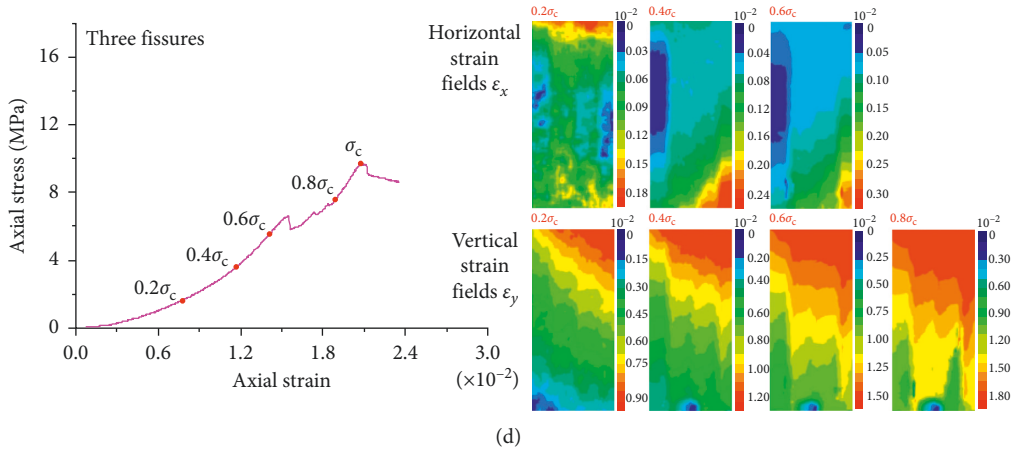

Figure 7: Deformation fields of specimens before peak stress: (a) intact specimens, (b) one fissure specimen, (c) two fissure specimens, and (d) three fissure specimens.

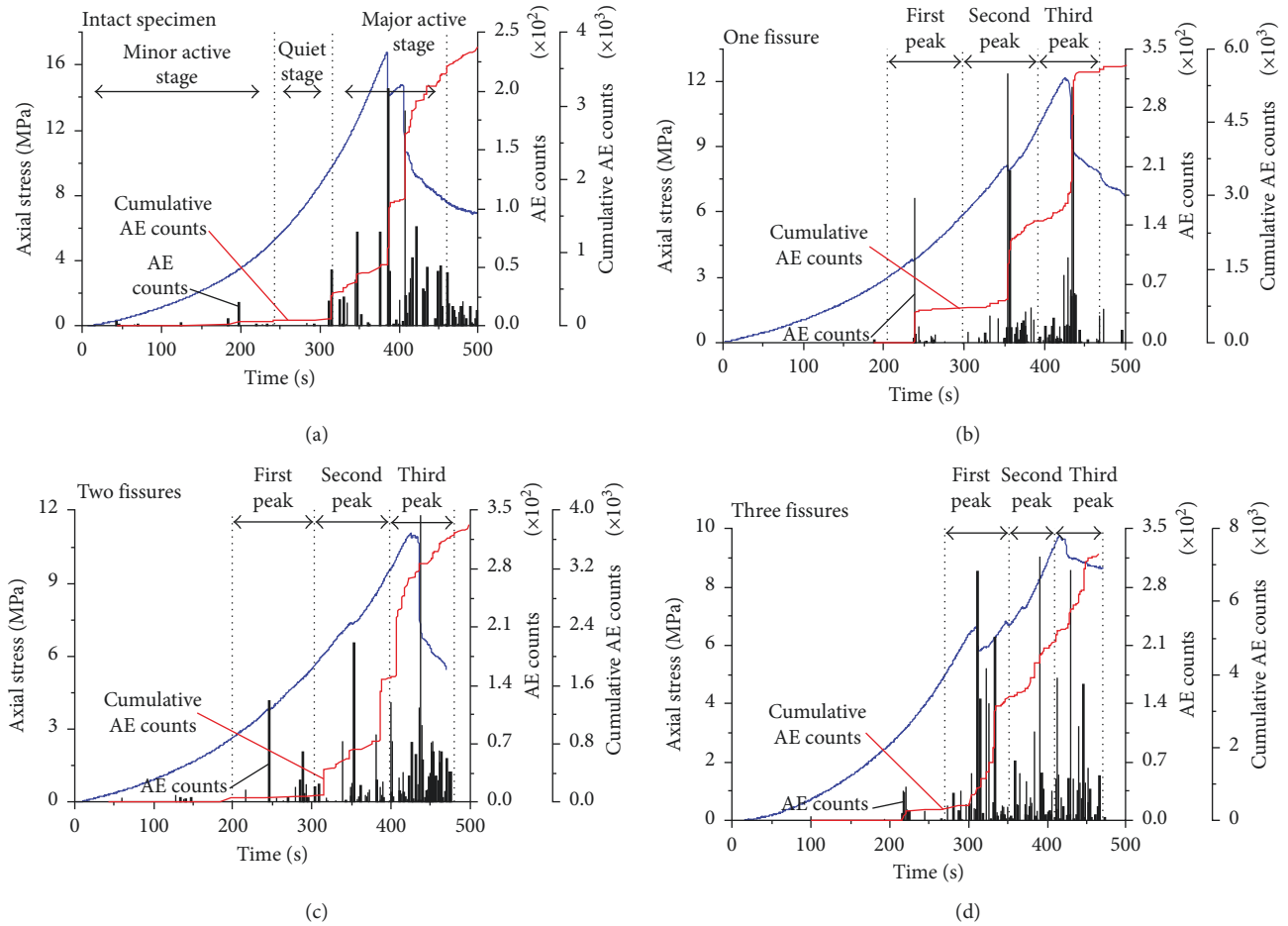

Figure 8: AE characteristics of specimens during the uniaxial loading process: (a) intact specimen, (b) one fissure specimen, (c) two fissure specimens, and (d) three fissure specimens.

stress. In general, the experimental results in Section 3 reveal two apparent reasons causing the dynamic instability of layer-crack structure, that is, the nonuniform deformation and the asymmetric load of supporting bodies. Therefore, the failure mechanism of layer-crack structure can be explained from the point of nonuniform deformation and asymmetric load.

As shown in Figure 10, a simple failure mechanism of layer-crack structure is established under the uniaxial

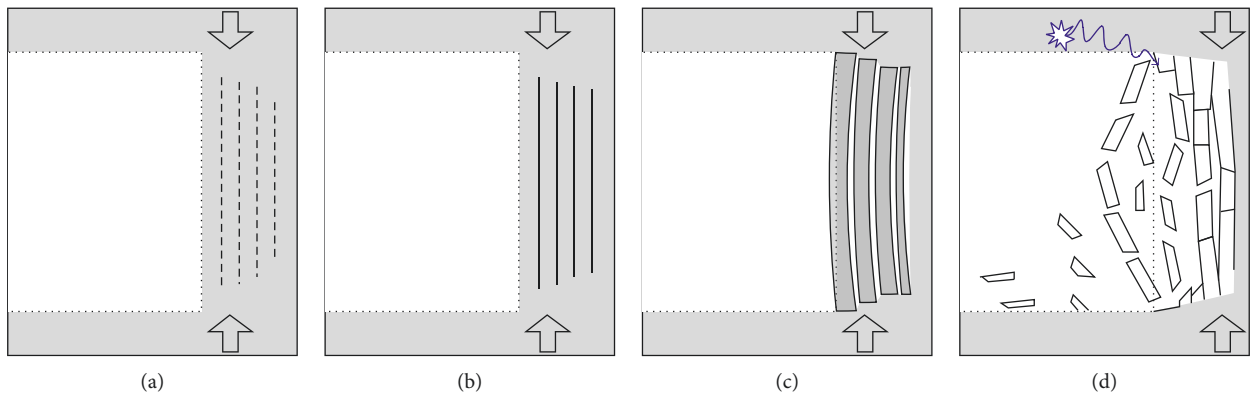

Figure 9: Schematic diagram of the occurrence mechanism of rock burst: (a) crack initiation and propagation, (b) formation of the layer-crack structure, (c) strain energy accumulation, and (d) occurrence of dynamic instability.

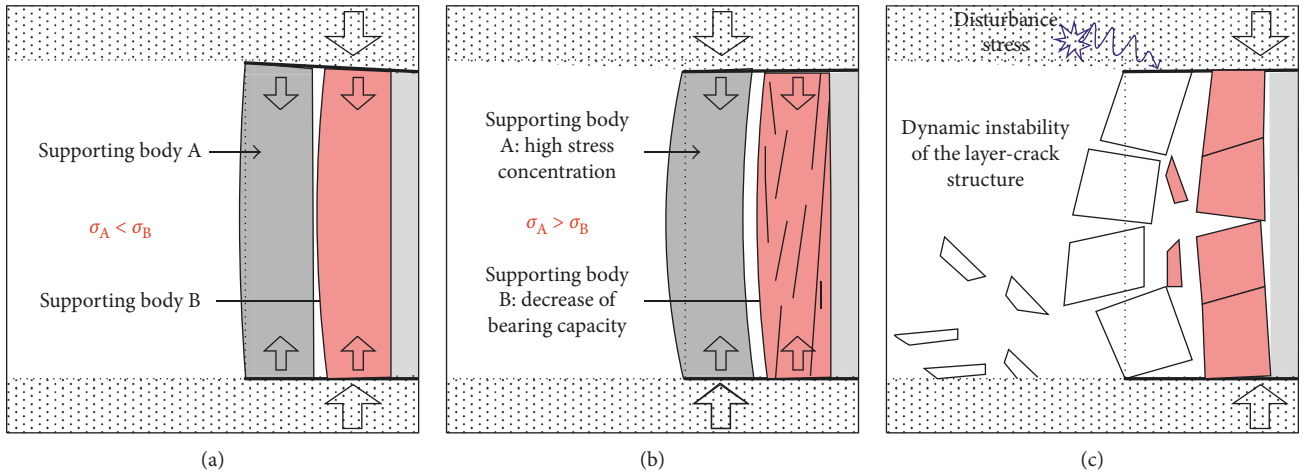

Figure 10: Schematic diagram of the failure mechanism of layer-crack structure: (a) under compression concentrating condition, (b) yield failure of supporting body B, and (c) dynamic instability of the whole layer-crack structure.

compression condition. Based on Figure 6, we have known that the failure of each supporting body of layer-crack specimens is stochastic, and thus assuming that the strain of supporting body B is larger than that of the supporting body A in Figure 10(a), that is, the stress σ_B acting on the supporting body B is larger than that σ_A acting on the supporting body A. As the compression stress continues concentrating, the supporting body B enters into the yield failure first while the supporting body A does not reach its limit bearing capacity. That is to say, the whole layer-crack structure still has a good bearing capacity, as shown in Figure 10(b). At the same time, the stress concentration degree of supporting body A increases rapidly due to the decrease of bearing capacity of supporting body B. The stress concentration exerted on the whole layer-crack structure mainly transfers onto the supporting body A. Consequently, a large stress gradient difference exists among the supporting bodies A and B. When the supporting body A reaches its limit bearing capacity, dynamic instability of the whole layer-crack structure will occur under the influence of disturbance stress, as shown in Figure 10(c). The failure mechanism of layer-crack structure containing more than two supporting bodies is similar.

Furthermore, the fissure number (i.e., number of supporting bodies) also greatly affects the stability of layer-crack structure according to the experimental results. The bearing capacity of layer-crack structure decreases as the fissure number increases, which means that the occurrence risk of dynamic instability also increases if the number of supporting bodies increases under the same stress and lithology conditions. There are two main reasons causing this result. First, the appearing time of nonuniform deformation phenomenon decreases as the fissure number increases. Thus, one or more than two supporting bodies of the layer-crack structure will enter into the yield failure stage earlier. The stress concentration of supporting bodies, not coming into the yield failure stage, will be aggravated. Second, zones of stress gradient difference increase as the fissure number increases. That is to say, unstable zones in the layer-crack structure will increase. Therefore, if the fissure number of layer-crack structure increases, the occurrence risk of dynamic instability also increases.

Based on the analysis of the failure mechanism of layer-crack structure, it reveals that rock bursts induced by the layer-crack structure can be mitigated by reducing the

number of layer-crack plate, avoiding the incompatible deformation and asymmetric load, and decreasing the impact energy. Three guidelines for controlling rock bursts induced by the layer-crack structure are proposed. First, control the number of layer-crack plate by optimizing the support system. Second, make the deformation of the layer-crack structure more compatible by enhancing the bearing capacity of these layer-crack plates coming into the process of plastic deformation or yield failure. Third, decrease the strain energy stored in the mainly supporting layer-crack plates of layer-crack structure and in other possible energy provided bodies. Although preventing the formation of layer-crack structure is the best way for mitigating rock bursts, it is almost impossible. Thus, the three guidelines proposed in this section are rational. This paragraph only provides three guidelines, and there are still lots of work that needs to be done for finding out these suitable and applicable mitigation strategies, methods, and techniques, for mitigating rock bursts induced by the layer-crack structure.

5. Conclusions

In this study, the mechanical properties of layer-crack rock models with different fissure numbers were investigated with uniaxial compression tests based on the phenomenon that rock bursts generally occur in stress concentration areas where layer-crack structures often exist. During the experimental process, the DSCM and AE techniques were applied to record and analyze the deformation and failure processes. The following conclusions can be drawn:

(1) Compared with intact rock models, the bearing capacity, deformation field, and AE behavior of layer-crack rock models show a great difference. First, the bearing capacity of layer-crack rock models is lower. Second, the nonuniform deformation phenomenon exists from the elastic deformation stage to peak stress for layer-crack rock models during the compression process but does not appear from compaction stage to peak stress for intact rock models. Third, the AE behavior of intact rock models consists of three stages, that is, active stage, quiet stage, and major active stage, but for layer-crack rock models, the AE behavior patter is characterized by three peaks without quiet stage after the minor active stage.

(2) The failure modes of intact rock models and layer-crack rock models are similar. Splitting failure accompanied with local shear failure is the main failure mode for intact rock models. For layer-crack rock models, splitting failure or shear failure of one or more than two of the supporting bodies is the mail failure mode. In addition, the failure of each supporting body of layer-crack rock models is stochastic.

(3) The fissure number greatly affects the mechanical properties of layer-crack rock models. When the fissure number increases from one to three, the uniaxial compressive strength and elastic modulus decrease about 25.21% and 37.50%, respectively. Meanwhile, the appearing time of nonuniform deformation phenomenon in the specimen surface also decreases as the fissure number increases. For example, the nonuniform deformation phenomenon appears when the axial stress reaches at $0.4–0.6\sigma_c$ for one fissure specimen or two fissure specimens, but for three fissure specimens, this phenomenon appears at $0.2–0.4\sigma_c$. In aspect of AE behavior, the AE events are denser and denser with the increase of fissure number in each peak stage, especially in the first and second peak stages.

(4) The failure mechanism of layer-crack structure can be described as follows. First, as the compression stress continues concentrating, one or more than two of the supporting bodies enter into the yield failure first while the remaining supporting bodies still have a good bearing capacity. This result causes the rapid increase of local stress concentration degree in the layer-crack structure. At the same time, some zones of stress gradient difference also exist. Second, when the remaining supporting bodies reach their limit bearing capacity, dynamic instability of the whole layer-crack structure will occur under the influence of disturbance stress. Furthermore, if the number of supporting bodies increases, the occurrence risk of dynamic instability will be enhanced.

Conflicts of Interest

The authors declare that they have no conflicts of interest.

Acknowledgments

This research was financially supported by the State Key Research Development Program of China (no. 2016YFC0801401), National Natural Science Foundation of China (nos. 51674160, 51474137, and 51704181), Scientific Research Foundation of Shandong University of Science and Technology for Recruited Talents (no. 2017RCJJ014), Natural Science Foundation of Shandong Province (no. ZR2016EEB23), Science and Technology Program of Shandong Provience University (no. J15LH02), Tai'shan Scholar Engineering Construction Fund of Shandong Province of China (ts201511026), and Taishan Scholar Talent Team Support Plan for Advantaged & Unique Discipline Areas.

References

[1] Y. L. Tan, F. H. Yu, J. G. Ning, and T. B. Zhao, "Design and construction of entry retaining wall along a gob side under hard roof stratum," *International Journal of Rock Mechanics and Mining Sciences*, vol. 77, pp. 115–121, 2015.

[2] T. B. Zhao, W. Y. Guo, Y. L. Tan, Z. Zhang, and K. K. Cheng, "Research on the mechanics mechanism of rock burst for mining in the variable region of coal thickness," *Journal of China Coal Society*, vol. 41, no. 7, pp. 1659–1666, 2016.

[3] J. G. Ning, J. Wang, J. Q. Jiang, S. C. Hu, L. S. Jiang, and X. S. Liu, "Estimation of crack initiation and propagation thresholds of confined brittle coal specimens based on energy dissipation theory," *Rock Mechanics and Rock Engineering*, vol. 51, no. 1, pp. 119–134, 2018.

[4] G. C. Zhang, S. J. Liang, Y. L. Tan, F. X. Xie, S. Chen, and H. Jia, "Numerical modeling for longwall pillar design: a case

study from a typical longwall panel in China," *Journal of Geophysics and Engineering*, vol. 15, no. 1, pp. 121–134, 2018.

[5] W. P. Huang, Q. Yuan, Y. L. Tan et al., "An innovative support technology employing a concrete-filled steel tubular structure for a 1000-m-deep roadway in a high in situ stress field," *Tunnelling and Underground Space Technology*, vol. 73, pp. 26–36, 2018.

[6] Y. L. Tan, X. S. Liu, J. G. Ning, and Y. W. Lu, "In situ investigations on failure development of overlying strata induced by mining multiple coalseams," *Geotechnical Testing Journal*, vol. 40, no. 2, pp. 244–257, 2017.

[7] T. B. Zhao, W. Y. Guo, Y. L. Tan, Y. C. Yin, L. S. Cai, and J. F. Pan, "Case studies of rock bursts under complicated geological conditions during multi-seam mining at a depth of 800m," *Rock Mechanics and Rock Engineering*, pp. 1–26, 2018.

[8] L. J. Dong, W. Zou, X. B. Li, W. W. Shu, and Z. W. Wang, "Collaborative localization method using analytical and iterative solutions for microseismic/acoustic emission sources in the rockmass structure for underground mining," *Engineering Fracture Mechanics*, 2018, In press.

[9] T. B. Zhao, Z. Y. Zhang, Y. C. Yin, Y. L. Tan, and X. Q. Liu, "Ground control in mining steeply dipping coal seams by backfilling with waste rock," *Journal of the South African Institute of Mining and Metallurgy*, vol. 118, no. 1, pp. 15–26, 2018.

[10] L. J. Dong, D. Y. Sun, X. B. Li, and K. Du, "Theoretical and experimental studies of localization methodology for AE and microseismic sources without pre-measured wave velocity in mines," *IEEE Access*, vol. 5, pp. 16818–16828, 2017.

[11] Q. M. Gong, L. J. Yin, S. Y. Wu, J. Zhao, and Y. Ting, "Rock burst and slabbing failure and its influence on TBM excavation at headrace tunnels in Jinping II hydropower station," *Engineering Geology*, vol. 124, no. 1, pp. 98–108, 2012.

[12] H. Zhou, R. C. Xu, J. J. Lu, Q. F. Zhang, C. Q. Zhang, and F. Z. Meng, "Experimental study of instability destruction and crack propagation characteristics of slab failure model specimen," *Rock and Soil Mechanics*, vol. 36, no. 2, pp. 1–11, 2015.

[13] K. M. Mohamed, M. M. Murphy, H. E. Lawson, and T. Klemetti, "Analysis of the current rib support practices and techniques in U.S. coal mines," *International Journal of Mining Science and Technology*, vol. 26, no. 1, pp. 77–87, 2016.

[14] T. B. Zhao, W. Y. Guo, Y. L. Tan, C. P. Lu, and C. W. Wang, "Case histories of rock bursts under complicated geological conditions," *Bulletin of Engineering Geology and the Environment*, pp. 1–17, 2017.

[15] W. Y. Guo, T. B. Zhao, Y. L. Tan, F. H. Yu, S. C. Hu, and F. Q. Yang, "Progressive mitigation method of rock bursts under complicated geological conditions," *International Journal of Rock Mechanics and Mining Sciences*, vol. 96, pp. 11–22, 2017.

[16] T. R. Stacey, "A simple extension strain criterion for fracture of brittle rock," *International Journal of Rock Mechanics and Mining Sciences & Geomechanics Abstracts*, vol. 18, no. 6, pp. 469–474, 1981.

[17] Z. S. Hou, Q. M. Gong, and Z. H. Sun, "Primary failure types and their failure mechanisms of deep buried and intact marble in Jinping II hydropower station," *Chinese Journal of Rock Mechanics and Engineering*, vol. 30, no. 4, pp. 727–732, 2011.

[18] S. L. Qiu, X. T. Feng, C. Q. Zhang, and T. B. Xiang, "Estimation of rockburst wall-rock velocity invoked by slab flexure sources in deep tunnel," *Canadian Geotechnical Journal*, vol. 51, no. 5, pp. 520–539, 2014.

[19] L. Weng, X. B. Li, Z. L. Zhou, and K. X. Liu, "Occurrence mechanism and time-dependency effect of buckling rock burst," *Journal of Mining and Safety Engineering*, vol. 33, no. 1, pp. 172–178, 2016.

[20] M. Cai, "Influence of intermediate principal stress on rock fracturing and strength near excavation boundaries-Insight from numerical modeling," *International Journal of Rock Mechanics and Mining Sciences*, vol. 45, no. 5, pp. 763–772, 2008.

[21] C. Q. Zhang, H. Zhou, X. T. Feng, L. Xing, and S. L. Qiu, "Layered fracture induced by principal stress axes rotation in hard rock during tunnelling," *Materials Research Innovations*, vol. 15, no. 1, pp. S527–S530, 2011.

[22] M. C. He, J. L. Miao, J. D. Li, and C. G. Wang, "Experimental study on rockburst processes of granite specimen at great depth," *Chinese Journal of Rock Mechanics and Engineering*, vol. 26, no. 5, pp. 865–876, 2007.

[23] M. C. He, J. L. Miao, and J. L. Feng, "Rockburst process of limestone and its acoustic emission characteristics under true-triaxial unloading conditions," *International Journal of Rock Mechanics and Mining Sciences*, vol. 47, no. 2, pp. 286–298, 2011.

[24] X. G. Zhao, J. Wang, M. Cai et al., "Influence of unloading rate on the strainburst characteristics of Beishan granite under true-triaxial unloading conditions," *Rock Mechanics and Rock Engineering*, vol. 47, no. 2, pp. 467–483, 2014.

[25] K. Du, M. Tao, X. B. Li, and J. Zhou, "Experimental study of slabbing and rockburst induced by true-triaxial unloading and local dynamic disturbance," *Rock Mechanics and Rock Engineering*, vol. 49, no. 9, pp. 1–17, 2016.

[26] X. C. Zhang, X. X. Miao, M. H. Zhai, and T. Q. Yang, "Analysis on rockburts mechanics in Sanhejian Coal Mine," *Chinese Journal of Rock Mechanics and Engineering*, vol. 17, no. 5, pp. 508–513, 1998.

[27] X. C. Zhang, X. X. Miao, and T. Q. Yang, "The layer-crack-plate model and testing study of the rockbursts in mines," *Chinese Journal of Rock Mechanics and Engineering*, vol. 18, no. 5, pp. 497–502, 1999.

[28] W. H. Peng and A. H. Lu, "Numerical simulation of layered crack and failure of roadway surrounding rock under the action of stress wave," *Journal of Mining and Safety Engineering*, vol. 25, no. 2, pp. 213–216, 2008.

[29] Q. S. Bai, S. H. Tu, X. G. Zhang, C. Zhang, and Y. Yuan, "Numerical modeling on brittle failure of coal wall in longwall face—a case study," *Arabian Journal of Geosciences*, vol. 7, no. 12, pp. 5067–5080, 2014.

[30] Q. S. Liu, J. Xu, X. W. Liu, J. D. Jiang, and B. Liu, "The role of flaws on crack growth in rock-like material assessed by AE technique," *International Journal of Fracture*, vol. 193, no. 2, pp. 99–115, 2015.

[31] H. Zhou, R. C. Xu, J. J. Lu, C. Q. Zhang, F. Z. Meng, and Z. Shen, "Study on mechanisms and physical simulation experiment of slab buckling rockbursts in deep tunnel," *Chinese Journal of Rock Mechanics and Engineering*, vol. 34, no. S2, pp. 3658–3666, 2015.

[32] W. Y. Guo, Y. L. Tan, T. B. Zhao, X. M. Liu, Q. H. Gu, and S. C. Hu, "Compression creep characteristics and creep model establishment of gangue," *Geotechnical and Geological Engineering*, vol. 34, no. 4, pp. 1193–1198, 2016.

[33] T. B. Zhao, Y. C. Yin, Y. L. Tan, and Y. M. Song, "Deformation tests and failure process analysis of an anchorage structure," *International Journal of Mining Science and Technology*, vol. 25, no. 2, pp. 237–242, 2015.

[34] M. S. Diederichs, "The 2003 Canadian geotechnical colloquium: mechanistic interpretation and practical application

of damage and spalling prediction criteria for deep tunnelling," *Canadian Geotechnical Journal*, vol. 44, no. 9, pp. 1082–1116, 2007.

[35] F. Z. Meng, H. Zhou, Z. Q. Wang et al., "Experimental study on the prediction of rockburst hazards induced by dynamic structural plane shearing in deeply buried hard rock tunnels," *International Journal of Rock Mechanics and Mining Sciences*, vol. 86, pp. 210–223, 2016.

[36] C. Q. Zhang, T. FengX, H. Zhou, S. L. Qiu, and W. P. Wu, "Case histories of four extremely intense rockbursts in deep tunnels," *Rock Mechanics and Rock Engineering*, vol. 45, no. 3, pp. 275–288, 2012.

[37] H. Zhou, F. Z. Meng, C. Q. Zhang, D. W. Hu, F. J. Yang, and J. J. Lu, "Analysis of rockburst mechanisms induced by structural planes in deep tunnels," *Bulletin of Engineering Geology and the Environment*, vol. 74, no. 4, pp. 1435–1451, 2015.

[38] M. Cai, "Principles of rock support in burst-prone ground," *Tunnelling and Underground Space Technology*, vol. 36, no. 6, pp. 46–56, 2013.

[39] W. D. Ortlepp and T. R. Stacey, "Rockburst mechanisms in tunnels and shafts," *Tunnelling and Underground Space Technology*, vol. 9, no. 1, pp. 59–65, 1994.

[40] W. D. Ortlepp and T. R. Stacey, "Performance of tunnel support under large deformation static and dynamic loading," *Tunnelling and Underground Space Technology*, vol. 13, no. 1, pp. 15–21, 1998.

[41] T. B. Zhao, W. Y. Guo, Y. L. Tan, F. H. Yu, B. Huang, and L. S. Zhang, "Failure mechanism of layer-crack rock models with different vertical fissure geometric configurations under uniaxial compression," *Advances in Mechanical Engineering*, vol. 9, no. 11, pp. 1–15, 2017.

[42] A. Dyskin and L. N. Germanovich, *Model of Rock Burst Caused by Cracks Growing Near Free Surface*, pp. 169–174, A. A. Balkema Publishers, Rotterdam, Netherlands, 1993.